Inorg. Chem. **2004**, *43*, 7764–7773

New Family of Lithium Salts for Highly Conductive Nonaqueous Electrolytes

Thomas J. Barbarich,*,† Peter F. Driscoll,† Suzette Izquierdo,† Lev N. Zakharov,‡ Christopher D. Incarvito,‡ and Arnold L. Rheingold‡

Yardney Technical Products, 82 Mechanic Street, Pawcatuck, Connecticut 06379, and Department of Chemistry and Biochemistry, University of California—San Diego, San Diego, California 92093

Received May 12, 2004

New lithium salts of weakly coordinating anions were prepared by treating lithium imidazolates or $LiN(CH_3)_2$ with 2 equiv of BF_3. They are $LiIm(BF_3)_2$, Li 2-MeIm$(BF_3)_2$, Li 4-MeIm$(BF_3)_2$, LiBenzIm$(BF_3)_2$, Li 2-^{i}PrIm$(BF_3)_2$, and $LiN(CH_3)_2(BF_3)_2$ (Im = imidazolate, Me = methyl, ^{i}Pr = isopropyl, BenzIm = benzoimidazolate). The salts were characterized by NMR spectroscopy and mass spectrometry. The structure of LiBenzIm$(BF_3)_2$ consists of a dimeric centrosymmetric unit with each lithium atom forming a bridge between the two anions through one fluorine contact to each anion. The structure of a hydrate of $LiN(CH_3)_2(BF_3)_2$ consists of an infinite chain in which each anion chelates two different lithium atoms through Li–F bonds. The conductivities of electrolyte solutions of these salts were measured and are discussed in terms of different ion-pairing modes determined from the solid-state structures, the anion's ability to distribute charge, and solution viscosity. Organic carbonate solutions of $LiIm(BF_3)_2$ partially disproportionate at 85 °C forming $LiBF_4$, $LiBF_2[Im(BF_3)]_2$, and Li[(BF_3)ImBF$_2$ImBF$_2$Im(BF_3)], reaching equilibrium by 3 months at 85 °C but not disproportionating at room temperature after 9 months. A mechanism for the formation of these disproportionation products is proposed. The lower conductivity of the 1 M $LiIm(BF_3)_2$ solution that has undergone disproportionation is attributed to the formation $LiBF_4$, which is less conductive, and $LiBF_2[Im(BF_3)]_2$ and Li[(BF_3)ImBF$_2$ImBF$_2$Im(BF_3)], which increase solution viscosity.

Introduction

Much of the effort devoted to the development and study of new weakly coordinating anions (WCAs) has been driven by their applications in catalysis and the study of unusual bonding in very reactive species with sites of virtual coordinative unsaturation.[1] In addition to these applications, lithium salts of WCAs are used to prepare organic electrolyte solutions for lithium-ion (Li-ion) batteries. These salts are used because the conductivity of the electrolyte is partially determined by the Li salt's ability to avoid ion-pair formation, a condition that reduces the effective number of charge carriers and lowers the conductivity. However, because the conductivity of the electrolyte is also determined by the viscosity of the solution, which generally increases with anion size, another goal in searching for new Li salts is to develop small anions, in direct contrast to recent attempts to prepare WCAs for catalytic applications.[2] Most recent efforts to develop new lithium salts for Li-ion batteries have focused on various lithium borates,[3] sulfonoimides,[4] methides,[5] and phosphates.[6]

Recently, a new family of weakly coordinating anions characterized by a monoanionic species with multiple Lewis

* Author to whom correspondence should be addressed. E-mail: tbarbarich@lithion.com.

† Yardney Technical Products.

‡ University of California—San Diego.

(1) (a) Strauss, S. H. *Chem. Rev.* **1993**, *93*, 927. (b) Reed, C. A. *Acc. Chem. Res.* **1998**, *31*, 133. (c) Piers, W. E. *Chem.—Eur. J.* **1998**, *4*, 13. (d) Chen, E. Y. X.; Marks, T. J. *Chem. Rev.* **2000**, *100*, 1391.

(2) Jia, L.; Yang, X.; Ishihara, A.; Marks, T. J. *Organometallics* **1995**, *14*, 3135.

(3) (a) Lishka, U.; Wietelmann, U.; Wegner, M. German Patent DE 19829030 C1, 1999. (b) Xu, W.; Angell, C. A. *Electrochem. Solid-State Lett.* **2001**, *4*, E1. (c) Barthel, J.; Buestrich, R.; Carl, E.; Gores, H. J. *J. Electrochem. Soc.* **1996**, *143*, 3572. (d) Barthel, J.; Buestrich, R.; Gores, H. J.; Schmidt, M.; Wuhr, M. *J. Electrochem. Soc.* **1997**, *144*, 3866. (e) Barthel, J.; Schmidt, M.; Gores, H. J. *J. Electrochem. Soc.* **1998**, *145*, L17. (f) Yamaguchi, H.; Takahashi, H.; Kato, M.; Arai, J. *J. Electrochem. Soc.* **2003**, *150*, A312. (g) Schmidt, M.; Kühner, A.; Franz, K.; Röschenthaler, G.; Kolomeitsev, A.; Kadyrov, A. European Patent 1,229,038A1, December 12, 2001. (h) Nolan, B. G.; Strauss, S. H. *J. Electrochem. Soc.* **2003**, *150*, A1726.

(4) (a) Armand, M.; Gauthier, M.; Muller, D. U.S. Patent 5,021,308, June 4, 1991. (b) Kita, K.; Kawakami, A.; Nie, J.; Sonoda, T.; Kobayashi, H. *J. Power Sources* **1997**, *68*, 307.

(5) Dominey, L. A. U.S. Patent 5,273,840, December 28, 1993.

10.1021/ic040070x CCC: $27.50
Published on Web 10/29/2004

base sites that are fully complexed by multiple Lewis acids was developed by LaPointe et al. for catalytic applications.[7] An example of this class of anions is $Im(B(C_6F_5)_3)_2^-$ (Im = imidazolate, $C_3N_2H_3$), shown below. Although these anions are very weakly coordinating as demonstrated by the effectiveness of ammonium salts as activators for olefin polymerization when combined with a titanocene catalyst, their corresponding Li salts are not appropriate for Li-ion batteries. This is because the large size of the anions results in highly viscous solutions that limit ion mobility and conductivity at the high Li salt concentrations used in Li-ion battery electrolyte solutions. Our approach to developing highly conductive, low cost lithium salts for Li-ion batteries is to choose a smaller, less expensive Lewis acid such as BF_3.

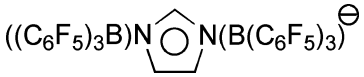

We have recently reported the conductivity, electrochemical stability, and initial cell cycling data for $LiIm(BF_3)_2$,[8] which is a new salt that incorporates this new class of WCAs. We have since obtained 900 cycles from cells containing this salt with a fade rate similar to that of cells containing $LiPF_6$, which is the current state of the art.[9] This paper describes the synthesis and conductivity for a series of these new salts. Structural analysis of the salts has yielded information about probable contact ion pairs in electrolyte solutions that can explain differences in conductivity. The thermal stability of the salts has also been investigated. The products of thermal decomposition in an electrolyte solution have been identified, and a mechanism for their formation is proposed. The conductivity of a solution stored at elevated temperatures for an extended period of time was measured, and the effect of the decomposition products on the electrolyte's conductivity is discussed.

Experimental Section

All preparations and physical measurements were carried out with the rigorous exclusion of air and water. Schlenk and glovebox techniques were employed with purified argon used as an inert gas when required. All reagents and solvents were reagent grade or better. Imidazole (ImH), benzimidazole (BenzImH), 2-methylimidazole (2-MeImH), 4-methylimidazole (4-MeImH), 2-isopropylimidazole (2-^{i}PrImH), and lithium dimethylamide were all purchased from Aldrich and used as received. Boron trifluoride diethyl etherate was purchased from Alfa Aesar and used as received. The following solvents were dried by distillation from the indicated drying agent: dichloromethane (P_2O_5), toluene (Na), and acetone (4-Å molecular sieves). Ethylmethyl carbonate (EMC; <30 ppm H_2O), ethylene carbonate (EC; <30 ppm H_2O), diethyl carbonate (DEC; <15 ppm H_2O), and dimethyl carbonate (DMC; <15 ppm H_2O) were purchased from EM Science and used as received.

NMR spectra were recorded using a Varian Unity Inova 500-MHz or a JEOL GSX 400-MHz NMR spectrometer. Chemical shifts (δ) are relative to $Si(CH_3)_4$ ($\delta = 0$ for ^{1}H NMR) and $CFCl_3$ ($\delta = 0$ for ^{19}F NMR). Chemical shifts for ^{11}B were externally referenced to $BF_3(Et_2O)$ in benzene-d_6 ($\delta = 0$ for ^{11}B NMR). Negative- and positive-ion electrospray mass spectra were performed on a Micromass Quattro II with cone voltages ranging from 15 to 70 V. A 10-μL aliquot was injected into a Rheodyne injector with an acetonitrile flow. Differential scanning calorimetry (DSC) was carried out on a TA Instruments DSC2010. Samples for DSC were prepared inside a glovebox, hermetically sealed in Al pans, and heated from room temperature to 300 °C at 5 °C/min.

Conductivities were measured using a Metrohm 712 conductivity meter. The cell assembly consisted of an Orion 018010 or a Metrohm 712 conductivity cell, which has platinized platinum electrodes with a cell constant of about 1 cm^{-1}. Cells were filled and sealed inside a glovebox under an argon atmosphere. The measurement temperatures were controlled to within 1 °C using a Tenney Environmental temperature chamber. The EC/EMC (1/3 by weight) and EC/DEC/DMC (1/1/1 by weight) solvent mixtures are representative of the solvents used in commercial Li-ion batteries. Viscosity measurements were made using a Cannon-Fenske viscometer. The temperature of the viscometer was controlled to within 1 °C by water from a Lauda Econline RE106 low-temperature circulator through copper coils that were submerged in an ethylene glycol bath with the viscometer.

Lithium Imidazolate. Both substituted and unsubstituted lithium imidazolates can be prepared by adding a small excess of *n*-BuLi to the appropriate imidazole in toluene. Substituted imidazoles have greater solubility, so the addition of the *n*-BuLi solution to the slurry containing substituted imidazoles was conducted at 0 °C because the reaction is exothermic. Reaction times varied from 1 to 2 days with reactions using substituted imidazoles generally being complete after 1 day. Yields were nearly quantitative. A representative preparation of unsubstituted lithium imidazolate is described. A slurry of imidazole (5.00 g, 73.5 mmol) in toluene (50 mL) was treated with 28 mL of a 2.65 M *n*-BuLi (74.2 mmol) solution in hexanes. This solution mixture was then refluxed for 2 days during which time the slurry became an off-white color. The slurry was then filtered over a medium glass frit, and the solid was washed with two 10-mL portions of toluene and then dried under vacuum to yield an off-white powder. Yield: 5.40 g, 99.4%.

Lithium Bis(trifluoroborane)imidazolate ($Li(BF_3)_2C_3H_3N_2$). A slurry of lithium imidazolate (5.00 g, 67.6 mmol) in CH_2Cl_2 (100 mL) at room temperature was treated with $BF_3(Et_2O)$ (19.6 mL, 154 mmol), and the mixture was refluxed for 2 days, during which time the slurry became yellow. The solid was then dried under vacuum to yield an off-white solid. Yield: 13.77 g, 97.1%. The solid was then dissolved in a minimal amount of EMC and filtered. Dichloromethane was added to this filtrate, and a precipitate formed. This precipitate was collected and dried under vacuum. Yield: 8.63 g, 61%. ^{1}H NMR (acetone-d_6): δ 7.87 (singlet, 1H), 7.08 (singlet, 2H). ^{19}F NMR (acetone-d_6): δ −147.5 (quartet, $J_{B-F} = 13$ Hz).

(6) (a) Schmidt, M.; Heider, A.; Kuehner, A.; Oesten, R.; Jungnitz, M.; Ignat'ev, N.; Sartori, P. *J. Power Sources* **2001**, *97*−*98*, 557. (b) Handa, M.; Suzuki, M.; Suzuki, J.; Kanamatsu, H.; Sasaki, Y. *Electrochem. Solid-State Lett.* **1999**, *2*, 60−62. (c) Gnanaraj, J. S.; Levi, M. D.; Gofer, Y.; Aurbach, D.; Schmidt, M. *J. Electrochem. Soc.* **2003**, *150*, A445. (d) Wietelmann, U.; Schade, K.; Lischka, U. PCT WO01/07450, February 1, 2001.

(7) LaPointe, R.; Roof, R. R.; Abboud, K. A.; Klosin, J. *J. Am. Chem. Soc.* **2000**, *122*, 9560.

(8) (a) Barbarich, T. J., Abraham, K. M.; DiCarlo, J. *Proceedings of the 40th Power Sources Conference*, June 10−13, 2002; IEEE: Cherry Hill, NJ; p331. (b) Barbarich, T. J.; Driscoll, P. *Electrochem. Solid-State Lett.* **2003**, *6*, A113. (c) Barbarich, T. J.; Ravdel, B.; Santee, S.; DiCarlo, J.; Abraham, K. M. *Proceedings of the 41st Power Sources Conference*, June 14−17, 2004; IEEE: Philadelphia, PA; p524. (d) Barbarich, T. J. PCT Int. Patent Appl. 10/289, 784, 2002.

(9) Ehrlich, G. M.; Lithium-Ion Batteries. In *Handbook of Batteries*, 3rd ed.; Linden, D., Reddy, T. B., Eds.; McGraw-Hill: New York, 2002; pp 35.21−35.28.

^{11}B NMR (acetone-d_6): δ 4.3 (quartet, J_{B-F} = 13 Hz). Low-resolution mass spectrum (negative-ion electrospray, acetone solution) Calcd for $C_3H_3N_2B_2F_6$: 203. Found *m*/*z*: 203 [(M-Li)]$^-$.

Lithium Bis(trifluoroborane)-2-methylimidazolate (Li(BF$_3$)$_2$C$_4$H$_5$N$_2$). A slurry of lithium 2-methylimidazolate (4.00 g, 45.5 mmol) in CH_2Cl_2 (70 mL) at 0 °C was treated with $BF_3(Et_2O)$ (11.7 mL, 93.2 mmol), and the mixture was refluxed for 3 days, during which time the slurry became yellow. The solid was then dried under vacuum to yield an off-white solid. Yield: 9.76 g, 96.0%. The solid was then dissolved in about 15 mL of DMC and filtered. Dichloromethane was added to this filtrate and a precipitate formed. This precipitate was collected and dried under vacuum. Yield: 7.34 g, 72.2%. ^{1}H NMR (acetone-d_6): δ 6.93 (singlet, 2H), 2.50 (singlet, 3H). ^{19}F NMR (acetone-d_6): δ −146.0 (quartet, J_{B-F} = 14 Hz). ^{11}B NMR (acetone-d_6): δ 4.4 (quartet, J_{B-F} = 13 Hz). Low-resolution mass spectrum (negative-ion electrospray, acetone solution): Calcd for $C_4H_5N_2B_2F_6$: 217. Found *m*/*z*: 217 [(M-Li)]$^-$.

Lithium Bis(trifluoroborane)-4-methylimidazolate (Li(BF$_3$)$_2$C$_4$H$_5$N$_2$). A slurry of lithium 4-methylimidazolate (4.00 g, 45.5 mmol) in CH_2Cl_2 (70 mL) at 0 °C was treated with $BF_3(Et_2O)$ (11.7 mL, 93.2 mmol), and the mixture was refluxed for 3 days, during which time the slurry became yellow. The solid was then dried under vacuum to yield an off-white solid. Yield: 9.10 g, 89.6%. The solid was then dissolved in about 15 mL of DMC and filtered. Dichloromethane was added to this filtrate, and a precipitate formed. This precipitate was collected and dried under vacuum. Yield: 6.80 g, 66.9%. ^{1}H NMR (acetone-d_6): δ 7.77 (singlet, 1H), δ6.79 (singlet, 1H), 3.71 (singlet, 3H). ^{19}F NMR (acetone-d_6): δ −146.6 (quartet, J_{B-F} = 14 Hz, 3F), δ −148.0 (quartet, J_{B-F} = 14 Hz, 3F). ^{11}B NMR (acetone-d_6): δ 4.3 (overlapping quartets). Low-resolution mass spectrum (negative-ion electrospray, acetone solution): Calcd for $C_4H_5N_2B_2F_6$: 217. Found *m*/*z*: 217 [(M-Li)]$^-$.

Lithium bis(trifluoroborane)-2-isopropylimidazolate (Li(BF$_3$)$_2$C$_6$H$_9$N$_2$). A slurry of lithium 2-methylimidazolate (4.00 g, 34.4 mmol) in CH_2Cl_2 (100 mL) at 0 °C was treated with $BF_3(Et_2O)$ (9.2 mL, 72.6 mmol), and the mixture was refluxed for 3 days, during which time the slurry became yellow. The solid was then dried under vacuum to yield an off-white solid. The solid was then dissolved in about 10 mL of DMC and filtered. Dichloromethane was added to this filtrate, and a precipitate formed. This precipitate was collected and dried under vacuum. Yield: 6.44 g, 58.6%. ^{1}H NMR (acetone-d_6): δ 6.96 (singlet, 2H), δ3.78 (septet, J_{H-H} = 7 Hz, 1H), 3.71 (doublet, J_{H-H} = 7 Hz, 6H). ^{19}F NMR (acetone-d_6): δ −143.2 (quartet, J_{B-F} = 14 Hz). ^{11}B NMR (acetone-d_6): δ 4.3 (quartet, J_{B-F} = 13 Hz). ^{11}B NMR (acetone-d_6): δ 4.4 (quartet, J_{B-F} = 13 Hz). Low-resolution mass spectrum (negative-ion electrospray, acetone solution): Calcd for $C_4H_5N_2B_2F_6$: 245. Found *m*/*z*: 245 [(M-Li)]$^-$.

Lithium Bis(trifluoroborane)benzimidazolate (Li(BF$_3$)$_2$C$_7$H$_5$N$_2$). A slurry of lithium benzimidazolate (8.25 g, 66.42 mmol) in CH_2Cl_2 (100 mL) at room temperature was treated with $BF_3(Et_2O)$ (17.5 mL, 138.1 mmol), and the mixture was refluxed for 3 days, during which time the slurry became gray. The solid was then dried under vacuum to yield an off-white solid. Yield: 16.14 g, 93.5%. The solid was then dissolved in a 1/3 EC/EMC and recrystallized. Yield: 13.93 g, 48.2% when the two ethylene carbonate molecules are accounted for in the crystal lattice. ^{1}H NMR (acetone-d_6): δ 8.35 (singlet, 1H), δ 7.83 (multiplet, 2H), 7.37 (multiplet, 2H). ^{19}F NMR (acetone-d_6): δ −146.3 (quartet, J_{B-F} = 14 Hz) spectrum. ^{11}B NMR (acetone-d_6): δ 4.8 (quartet, J_{B-F} = 13 Hz). Low-resolution mass spectrum (negative-ion electrospray, acetone solution): Calcd for $C_7H_5N_2B_2F_6$: 253. Found *m*/*z*: 253 [(M-Li)]$^-$.

Table 1. Crystal Data and Structure Refinement Details

compound	$[LiBenzIm(BF_3)_2\cdot 2EC)]_2$	$[LiN(CH_3)_2(BF_3)_2\cdot H_2O]_n$
formula	$C_{26}H_{26}B_4F_{12}Li_2N_4O_{12}$	$C_2H_8B_2F_6LiNO$
formula weight	871.63	204.65
space group	$P\bar{1}$	*Cmcm*
a, Å	8.24(3)	9.0878(10)
b, Å	9.40(4)	11.4667(13)
c, Å	12.17(5)	7.5549(9)
α, deg	96.28(9)	90
β, deg	91.71(9)	90
γ, deg	109.51(8)	90
V, Å^3	881(6)	787.27(16)
Z, *Z*′	1, 0.5	4, 0.25
crystal color, habit	colorless, plate	colorless, block
D(calcd), g cm^{-3}	1.643	1.727
μ(Mo Kα), cm^{-1}	1.63	2.06
temp, K	223(2)	100(2)
radiation	Mo Kα (*λ* = 0.71073 Å)	Bruker Smart Apex CCD
no. collected	5780	2419
no ind.	3753 (R_{int} = 0.0364)	517 (R_{int} = 0.0183]
R(*F*), %[a]	6.27	2.52
R(*wF*^{2}),%[b]	16.87	6.67

[a] $R = \sum||F_o| - |F_c||/\sum|F_o|$, [b] $R(\omega F^2) = \{\sum[\omega(F_o^2 - F_c^2)^2]/\sum[\omega(F_o^2)^2]\}^{1/2}$; $\omega = 1/[\sigma^2(F_o^2) + (aP)^2 + bP]$, $P = [2F_c^2 + \max(F_o,0)]/3$.

Lithium Bis(trifluoroborane)dimethylamide (LiN(CH$_3$)$_2$(BF$_3$)$_2$). A slurry of lithium dimethylamide (1.367 g, 26.80 mmol) in toluene (100 mL) at −78 °C was treated with $BF_3(Et_2O)$ (17.5 mL, 138.1 mmol) dropwise through an addition funnel. On warming, the solution became bright white. The mixture was then refluxed for 3 days, during which time the slurry became off-white. The slurry was then filtered, and the solid was then dried under vacuum to yield an off-white solid. Yield: 4.26 g, 85.2%. ^{1}H NMR (acetone-d_6): δ 2.25 (singlet). ^{19}F NMR (acetone-d_6): δ −156.9 (quartet, J_{B-F} = 17 Hz) spectrum. ^{11}B NMR (acetone-d_6): δ 5.1 (quartet, J_{B-F} = 18 Hz). Low-resolution mass spectrum (negative-ion electrospray, acetone solution) Calculated for $C_2H_6NB_2F_6$: 180. Found *m*/*z*: 180 [(M-Li)]$^-$. X-ray diffraction quality crystals of a hydrate of this salt were formed at a crack in a vial containing a tetrahydrofuran solution of this salt.

X-ray Crystal Structure Determinations. Diffraction intensity data were collected with Siemens P4/CCD ($[LiBenzIm(BF_3)_2\cdot 2EC)]_2$) and Bruker SMART APEX CCD ($[LiN(CH_3)_2(BF_3)_2\cdot H_2O]_n$) diffractometers. Crystal data and structure refinement details are given in Table 1. The structures were solved using direct methods, completed by subsequent difference Fourier syntheses, and refined by full matrix least-squares procedures on F^2. SADABS[10] absorption corrections were applied to all data (T_{min}/T_{max} = 0.796 and 0.916, respectively, for $[LiBenzIm(BF_3)_2\cdot 2EC)]_2$ and $[LiN(CH_3)_2(BF_3)_2\cdot H_2O]_n$). All non-hydrogen atoms were refined with anisotropic displacement coefficients. Hydrogen atoms in $LiBenzIm(BF_3)_2\cdot 2EC)]_2$ were treated as idealized contributions. In $[LiN(CH_3)_2(BF_3)_2\cdot H_2O]_n$ they were found on the *F*-map and refined with isotropic thermal parameters. All software and sources of scattering factors are contained in the SHELXTL (5.10) program package (G. Sheldrick, Bruker XRD, Madison, WI).

Results and Discussion

The new Li salts prepared in this study were formed by the addition of 2 equiv of a Lewis acid to an anion having two Lewis base sites. The two-step synthesis of one of the salts prepared, lithium bis(trifluoroborane)imidazolate (LiIm-

(10) Sheldrick, G. M. *SADABS: Bruker/Siemens Area Detector Absorption Correction Program*, version 2.01; Bruker AXS: Madison, WI, 1998.

Chart 1

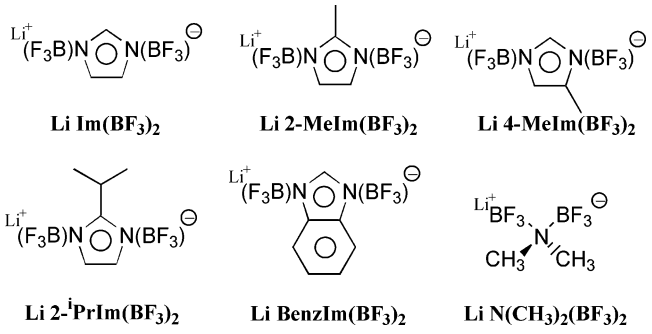

$(BF_3)_2$), is shown below in eqs 1 and 2. The overall preparation involves the addition of 2 moles of BF_3 to 1 mole of the Li salt of imidazole.

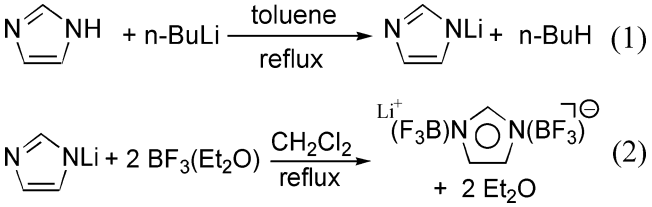

By use of this general method, the salts shown in Chart 1 have all been prepared from imidazole and its derivatives: 2-MeImH, 4-MeImH, 2-*i*PrImH, and BenzImH. The salt $LiN(CH_3)_2(BF_3)_2$ was prepared by the addition of $BF_3(Et_2O)$ to commercially available $LiN(CH_3)_2$ as shown in eq 3.

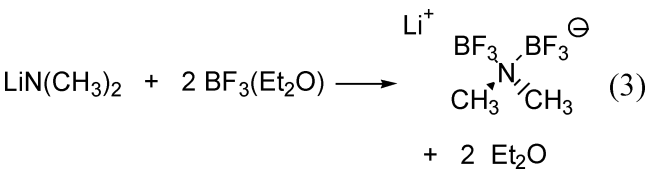

Purification of the salts of impurities that are harmful to lithium batteries was accomplished by dissolving the salts in a common electrolyte solvent, such as an organic carbonate, and filtering to remove unidentified insoluble impurities. With the exception of $LiBenzIm(BF_3)_2$, the salts were too soluble in organic carbonates for them to be precipitated by cooling a concentrated solution. Therefore, dichloromethane was added to these solutions to precipitate the Li salt that was then collected by filtration and vacuum dried. The second filtration removes the ether byproduct, which is difficult to remove under vacuum even at elevated temperatures probably because of the propensity of ether to coordinate to lithium ions. The organic carbonate displaces the ether from the lithium cation, and the ether, which remains in the organic carbonate/CH_2Cl_2 solution, is readily separated from the precipitated salt. The final product, after drying under vacuum, typically contains a small amount of organic carbonate.

The salts were characterized by NMR and mass spectrometry. With the exception of the anion 4-MeIm$(BF_3)_2^-$, the NMR spectra for all of the anions (see bottom spectra in Figures 6, 7, and 8 for the ^{11}B, ^{19}F, and ^1H NMR spectra of $LiIm(BF_3)_2$, respectively) are consistent with C_{2v} symmetry

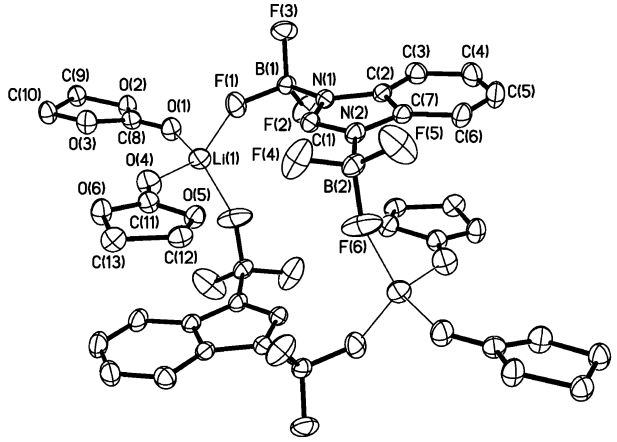

Figure 1. Structure of $[LiBenzIm(BF_3)_2 \cdot 2EC]_2$. Thermal ellipsoids are shown at the 30% level. Hydrogen atoms are omitted for clarity.

in acetone solution at room temperature, which indicates that the lithium cations either are not associated with the anion in an acetone solution or are involved in a rapid exchange between anions. The two most intense peaks in the negative-ion electrospray mass spectrum were those having the mass of the anion and the mass of the anion with loss of a BF_3 group. The ^{19}F and ^{11}B NMR spectra of these salts all show, in addition to the desired product, the presence of the BF_4^- anion that was identified by spiking an NMR sample with $LiBF_4$. A peak was also observed in the mass spectrum with a *m*/*z* of 87 Da and an isotope pattern that is consistent with the BF_4^- anion. Presumably, the counterion is the lithium cation, and because $LiBF_4$ is an electrochemically stable and conductive salt that has been used in lithium batteries, it was not removed from the desired salt. A small quantity of another impurity related to thermal decomposition (see below) was also detected in the ^1H NMR spectra for each of these compounds, but it does not appear to affect battery performance adversely.[8]

Structure of $[LiBenzIm(BF_3)_2 \cdot 2EC]_2$. The solid-state structure of $LiBenzIm(BF_3)_2$ provides a good example of a contact ion-paired species, a polar but nonionic solute, that might form in electrolyte solutions at high concentrations. As Figure 1 shows, $LiBenzIm(BF_3)_2$ crystallizes from a 1/3 EC/EMC electrolyte solution as a dimer with the two lithium cations bridging the anions through a fluorine atom on each BF_3 group. Two EC molecules are also coordinated to the lithium cation. The bond distances within the five-membered ring of the benzimidazole fragment are within experimental error of those in $Im(M(C_6F_5)_3)_2^-$ (M = B, Al)[7] with the exception of the C(2)−C(7) bond that is shared with the six-membered ring. The average B−N bond distance of 1.560 Å is somewhat shorter than the B−N bond distance of 1.585 Å in $Im(B(C_6F_5)_3)_2^-$.[7] Each of the BF_3 groups has one fluorine atom bonded to a lithium cation, with the B−F(Li) distances of 1.383(5) and 1.377(6) Å being slightly longer than the average terminal B−F bond distance of 1.356 Å.

The coordination sphere of the lithium cation can best be described as a distorted tetrahedron. Bond distances and angles are listed in Table 2. Each Li^+ cation is coordinated to one fluorine atom of each anion and is also bound to the

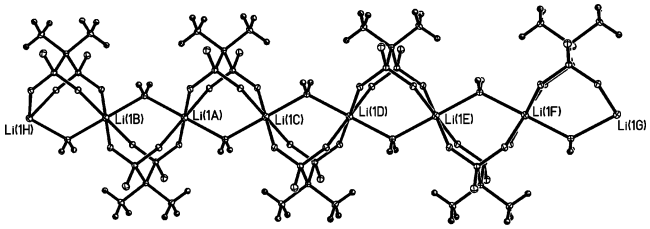

Figure 2. Structure of $[LiN(CH_3)_2(BF_3)_2{\cdot}H_2O)]_n$ showing the infinite chains formed from the interaction of the lithium cation with a water molecule and the anion.

Table 2. Selected Bond Lengths (Å) and Angles (deg) for $[LiBenzIm(BF_3)_2{\cdot}EC]_2$

Bond Lengths			
Li(1)−F(1)	1.897(8)	Li(1)−F(6′)	1.870(9)
Li(1)−O(1)	1.896(6)	Li(1)−O(4)	1.897(10)
B(1)−F(1)	1.383(5)	B(2)−F(4)	1.354(5)
B(1)−F(2)	1.363(5)	B(2)−F(5)	1.344(6)
B(1)−F(3)	1.362(5)	B(2)−F(6)	1.377(6)
B(1)−N(1)	1.569(5)	B(2)−N(2)	1.552(7)
O(1)−C(8)	1.199(5)	O(4)−C(11)	1.197(5)

Bond Angles			
F(1)−Li(1)−F(6′)	120.4(3)	F(1)−Li(1)−O(1)	109.0(3)
F(1)−Li(1)−O(4)	100.4(3)	O(1)−Li(1)−O(4)	115.3(3)
O(1)−Li(1)−F(6′)	107.1(3)	O(4)−Li(1)−F(6′)	104.9(3)
Li(1)−O(1)−C(8)	141.0(3)	Li(1)−O(4)−C(11)	137.4(3)
Li(1)−F(1)−B(1)	128.7(3)	Li(1′)−F(6)−B(2)	157.8(3)

carbonyl oxygen atoms of two EC solvent molecules. The Li−F(B) bond distances of 1.870(9) and 1.897(8) Å are virtually the same as the Li−O distances of 1.896(6) and 1.897(10) Å and are not unusual. By use of bond valence theory[11] to gauge the relative importance of the bonds in stabilizing the cation, one finds that the Li−F(B) bonds contribute 43.7% of the valence of the lithium cation compared to 56.3% for the Li−O bond formed from coordination to the ethylene carbonate solvent molecules. The high degree of stabilization suggests that the imidazole-based anions, which probably are capable of ion pairing in a similar manner because of their similar structure and chemistry to $LiBenzIm(BF_3)_2$, are able to compete effectively with solvent molecules for the lithium cations.

Structure of $[LiN(CH_3)_2(BF_3)_2{\cdot}H_2O)]_n$. The structure consists of infinite chains in which $LiN(CH_3)_2(BF_3)_2$ units are connected by H_2O molecules. As Figure 2 shows, the chain consists of zigzagging units such that the water molecule and the anion are on opposing sides of the line formed from the Li cations. In the other two dimensions, there is (O)H···F(B) hydrogen bonding between the hydrogen atoms of the water molecule and the F(2) atom of the BF_3 group of the anion. This hydrogen bonding is shown in Figure 3. The short (O)H···F(B) intermolecular bond distance of 1.93(2) Å and the nearly linear O−H···F bond angle of 174(2)° indicate that this interaction is significant. These hydrogen bonds undoubtedly add significantly to the stability of the crystal.

(11) (a) Brown, I. D. In *Structure and Bonding in Crystals*; O'Keefe, M., Navrotsky, A., Eds.; Academic Press: New York, 1981; Vol. 2, Chapter 14, p 1. (b) Brown, I. D.; Altermatt, D. *Acta Crystallogr.* **1985**, *B41*, 244. (c) O'Keefe, M. *Structure and Bonding*; Springer-Verlag: Berlin, 1989; Vol. 71, p 161.

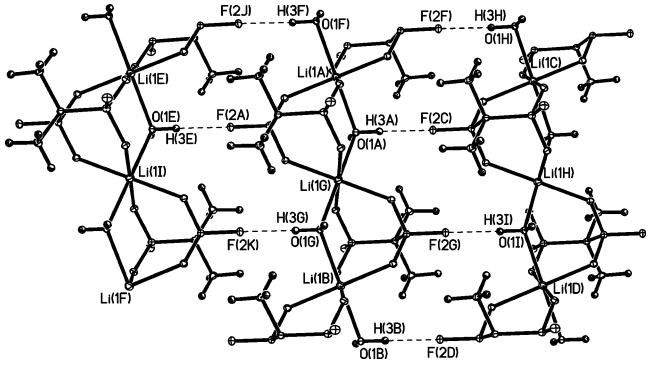

Figure 3. Structure of $[LiN(CH_3)_2(BF_3)_2{\cdot}H_2O)]_n$ showing the infinite chains formed from the hydrogen bonding (dashed lines) of the hydrogen atoms of the water molecule with the fluorine atoms of the BF_3 groups of the anion. A symmetrically equivalent chain is also going through the plane of the paper.

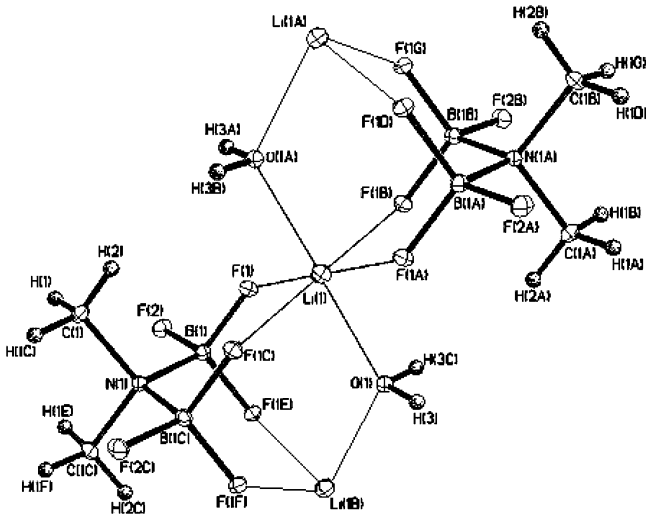

Figure 4. Structure of $[LiN(CH_3)_2(BF_3)_2{\cdot}H_2O)]_n$ showing the environment around the lithium cation. Thermal ellipsoids are shown at the 50% level.

The anion itself, Figure 4, consists of a nitrogen atom in a slightly distorted tetrahedral environment bonded to two methyl and two BF_3 groups. The B(1)−N(1)−B(1C) angle of 112.99(14)° is slightly larger than the 107.45(14)° bond angle for C(1)−N(1)−C(1C). The remaining C−N−B bond angles are 109.06(4)°. Each anion forms a bidentate chelate to two different lithium atoms through a pair of fluorine atoms with each of the fluorine atoms residing on different boron atoms. These chelates form a six-membered F−Li−F−B−N−B ring that adopts a chair formation. Two of the fluorine atoms of each BF_3 group are bonded to a Li^+ cation, whereas the remaining fluorine atom forms a hydrogen bond to a hydrogen atom of a water molecule. The 1.398(1) Å B−F(Li) bond distance is longer than the B−F(H) bond distance of 1.384(2) Å, suggesting a stronger interaction between the fluorine atom and the Li^+ cation than that between the fluorine atom and the hydrogen atom.

The structural environment of the Li^+ cation is also shown in Figure 4; selected bond lengths and angles are given in Table 3. The coordination sphere around the lithium cation consists of two pairs of fluorine atoms with each pair from a different anion and two contacts to oxygen atoms of water

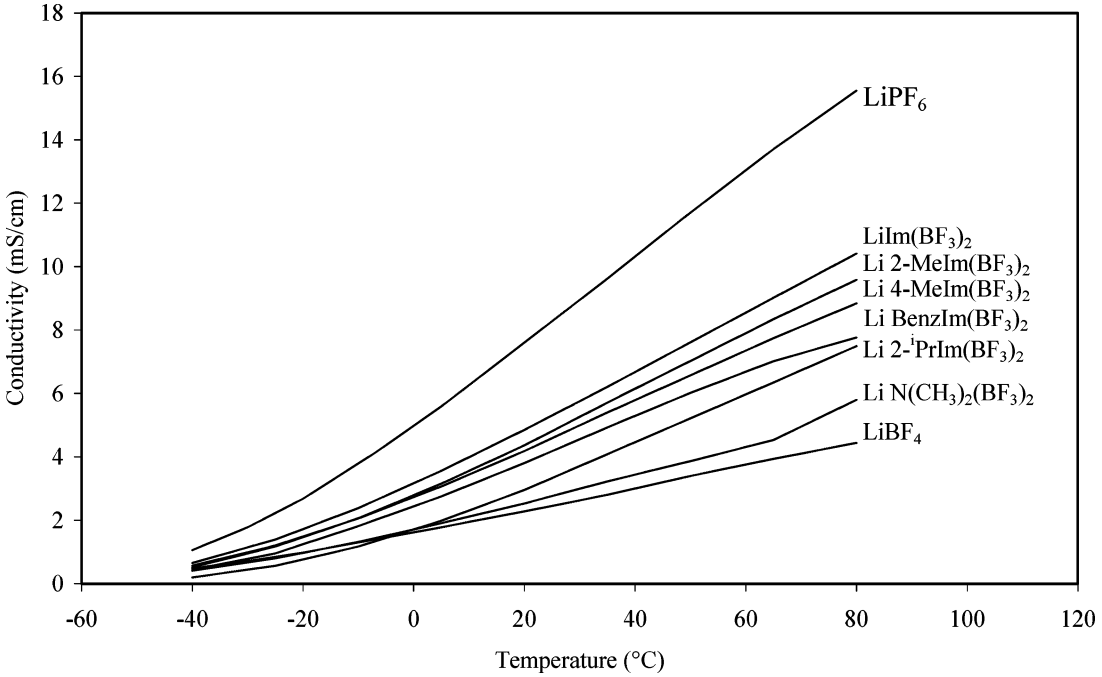

Figure 5. Conductivities of the new Li salt solutions in 1/3 EC/EMC (wt %) over the temperature range of −40 to +80 °C. With the exception of the solution containing LiBenzIm$(BF_3)_2$ which was 0.5 M, the concentration of the salts was 1 M. Solutions containing $LiPF_6$ and $LiBF_4$ are included for comparison.

molecules. The structure is best described as a distorted octahedron with the lithium and fluorine atoms forming the equatorial plane and the O−Li−O vector bisecting this plane at a 88.27(3)° angle. The oxygen atoms each form a bridge between two Li atoms, which forms two equivalent six-membered Li−O−Li−F−B−F rings. This coordination environment around lithium is unusual because there are only a few structures in which lithium is contacted by at least four fluorine atoms with additional contacts to other atoms.[12] The Li−F and Li−O bond distances of 2.0090(5) and 2.1334(7) Å, respectively, are comparable to those found in $LiBF_4(H_2O)$, which has Li−F bond distances of 2.025 and 2.115 Å and a Li−O bond distance of 2.109 Å.[13]

Conductivity. The conductivity of the salts was measured over the temperature range of −40 to +80 °C in 1/3 EC/EMC. The conductivity of $LiPF_6$, the current state-of-the-art salt for Li-ion batteries, is also shown in Figure 5 for comparison. Several of the new salts exhibit high conductivity, being more than twice that of $LiBF_4$ at 20 °C. Obviously $LiBF_4$, which is a minor contaminant, is not responsible for the high conductivity of these salts. The conductivities of the imidazole-based salts follow the trend unsubstituted imidazole > 2-methylimidazole > 4-methylimidazole > benzimidazole > 2-isopropylimidazole. Omitting the benzimidazole-based salt, where the conductivity was measured at 0.5 M (because of its lower solubility) instead of 1 M, the conductivity decreases with an increase in viscosity as Table 4 shows. This is expected because the degree of ion pairing between the anion and cation in these molecules is probably very similar because their structures and chemistry are also very similar. The conductivity of a solution containing the salt with the smallest mass, $LiN(CH_3)_2(BF_3)_2$, is the lowest of the salt solutions measured despite its lower viscosity. Clearly, the degree of ion pairing with this salt is greater than in the case of the imidazole-based salts. A 1 M $LiBF_4$ solution has an even lower conductivity than a 1 M $LiN(CH_3)_2(BF_3)_2$ solution despite its lower viscosity. Therefore, the degree of ion pairing in $LiBF_4$ solutions must be even greater.

Table 3. Selected Bond Lengths (Å) and Angles (deg) for $[LiN(CH_3)_2(BF_3)_2 \cdot H_2O)]_n$.

Bond Lengths			
Li(1)−F(1)	2.0090(5)	Li(1)−O(1)	2.1334(7)
B(1)−F(1)	1.3977(10)	B(1)−F(2)	1.3843(16)
B(1)−N(1)	1.5948(17)	O(1)−H(3)	0.86(2)
H(3)···F(2)′	1.93(2)	O(1)···F(2)′	2.783(1)
Bond Angles			
F(1)−Li(1)−F(1A)	180.0	F(1)−Li(1)−F(1B)	95.56(3)
F(1)−Li(1)−F(1C)	84.44(3)	F(1)−Li(1)−O(1)	88.27(3)
F(1)−Li(1)−O(1A)	91.73(3)	Li(1)−O(1)−Li(1B)	124.58(7)
Li(1)−F(1)−B(1)	131.47(7)	O(1)−H(3)−F(2)′	174(2)

Table 4. Conductivity, Viscosity, and Molecular Weight of Various 1 M Salt Solutions[a] in 1/3 EC/EMC (wt %) at 20 °C

salt (1 M in 1/3 EC/EMC)	conductivity (mS cm^{-1})	viscosity (cSt)[b]	molecular weight of salt (Da)
Li $Im(BF_3)_2$	4.86	3.09	209.6
Li 2-$MeIm(BF_3)_2$	4.37	3.13	223.6
Li 4-$MeIm(BF_3)_2$	4.18	3.20	223.6
Li 2-^{i}$PrIm(BF_3)_2$	2.95	4.61	251.7
Li $N(CH_3)_2(BF_3)_2$	2.54	2.49	186.6
Li BF_4	2.31	2.04	93.7

[a] Salt solutions contained some $LiBF_4$ as an impurity. (See the text.)

(12) (a) Guzei, I. A.; Radzewich, C. E.; Jordan, R. F. *Acta Crystallogr.* **2000**, *C56*, 279. (b) Barbarich, T. J.; Handy, T. S.; Miller, S. M.; Anderson, O. P. Grieco, P. A.; Strauss, S. H. *Organometallics* **1996**, *15*, 3776. (c) Kunzel, A.; Roesky, H. W.; Noltemeyer, M.; Schmidt, H.-G. *Chem. Commun.* **1995**, 2145.

(13) Shchegoleva, T. M.; 'Iskhakova, L. D.; Trunov, V. K. *Kristallografiya* **1986**, *31*, 1076.

Table 5. Decomposition Temperatures of the Various Salts Determined by DSC and Visual Observations

salt	DSC onset temperature	observation
Li $Im(BF_3)_2$	189	melted, bubbles
Li 2-$MeIm(BF_3)_2$	213	melted, bubbles
Li 4-$MeIm(BF_3)_2$	174	melted, bubbles
Li $BenzIm(BF_3)_2$	220	discoloration, loss of mass
Li 2-^{i}PrIm$(BF_3)_2$	237	discoloration, loss of mass
$LiN(CH_3)_2(BF_3)_2$	176	sublimation w/decomposition

An important question that still needs to be answered is, what governs the degree of ion pairing and the ultimately observed conductivity? For the salts $LiBF_4$ and $LiN(CH_3)_2(BF_3)_2$ and the imidazole-based salts, the lithium cation almost certainly forms contact ion pairs by forming bonds to the fluorine atoms of the anion as is observed in Figures 1 and 4. For each of these salts, the fluorine atoms to which the lithium cations binds are all part of a BF_3X ($X^- = F$, $N(CH_3)_2(BF_3)$, imidazole, substituted imidazole) unit. The degree of ion pairing will therefore be determined by the ability of X^- to delocalize the charge. The observed order of conductivity, imidazole-based salts > $LiN(CH_3)_2(BF_3)_2$ > $LiBF_4$ can be explained in terms of the lower-conductivity salts such as $LiBF_4$ having greater ion pairing, and thus a lower concentration of charge carriers, than the other more conductive salts. In the case of BF_4^-, the center of the charge is located on one boron atom that is surrounded by four electronegative fluorine atoms. The $N(CH_3)_2(BF_3)_2^-$ anion most likely has the majority of its negative charge distributed primarily over the nitrogen atom, two boron atoms, and six fluorine atoms. This delocalization of charge gives the salt a greater conductivity than $LiBF_4$ despite the more than 100% increase in mass and the associated increase in electrolyte viscosity. The imidazole-based anions are even more effective at distributing the negative charge over the entire molecule. In this anion, the charge is expected to be mostly spread over the entire aromatic ring and the two BF_3 groups, which are located on two separate nitrogen atoms, each of which have equal (or nearly equal for unsymmetrical imidazole rings) charge, thus lowering the Lewis basicity of the fluorine atoms. Pure electrostatic interactions are also decreased. Furthermore, differences in the modes in which the anion can interact with the cation can contribute to differences in the strength of the interaction of the anion with the cation. For example, the anion $N(CH_3)_2(BF_3)_2^-$ is able to chelate the lithium cation in the solid state as shown in Figure 4. In solution, the anion might also form a similar chelate to the lithium cation that should lead to a stronger interaction. The imidazole-based salts that have a different structural motif might not be able to chelate the lithium cation and thus do not form ion pairs that are as strong. The lower conductivity of the substituted imidazoles compared to that of the unsubstituted imidazole is presumably due to their increased mass and the resulting increased viscosity, because alkyl substitution is not likely to effect charge delocalization on the anion significantly.

Thermal Stability. Because the Li-ion cell cycle life at elevated temperatures can be dependent upon the stability of the salt, the thermal stability of the salts was investigated.

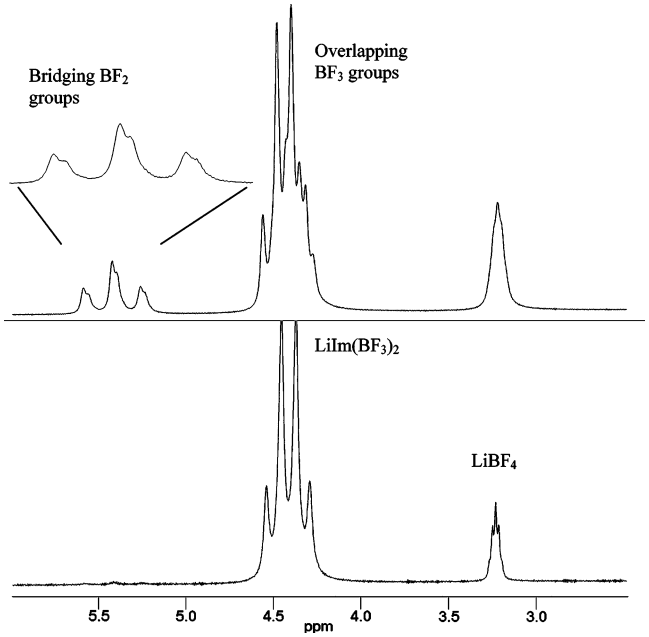

Figure 6. ^{11}B NMR spectra at 160.4 MHz of a 1 M $LiIm(BF_3)_2$ 1/1/1 EC/DMC/DEC solution before (bottom spectrum) and after (top spectrum) storage at 85 °C for 7 months in a sealed glass vial. The new species that forms after storage at 85°C (besides $LiBF_4$) has imidazole rings linked by BF_2 groups. Two overlapping triplets are observed, which shows that the two new species that have formed have BF_2 bridging groups.

Differential scanning calorimetry showed an endothermic decomposition process for each of the salts except Li 2-^{i}PrIm$(BF_3)_2$. The endothermic event was not due to a reversible melting process because repeating the DSC experiment on the sample did not yield similar results. The onset temperatures for the decomposition are given in Table 5. Visual observation of the salts in a sealed capillary tube in a melting-point apparatus showed that some of these some of these samples melted while others remained a solid but clearly lost mass and became discolored at approximately the same temperature as the process observed in the DSC data. Bubbles were observed in samples that melted, suggesting the evolution of gas. Thermal gravimetric analysis of $LiIm(BF_3)_2$ also showed a loss of mass beginning at approximately the same temperature as the endotherm in the DSC. These observations suggest gas evolution during decomposition, which is probably BF_3 gas.

The thermal stability of the parent salt, $LiIm(BF_3)_2$, in a solution was investigated by NMR spectroscopic and mass spectrometric analysis of samples stored for extended periods of time at elevated temperatures. A 1 M solution of this salt in a 1/1/1 EC/DMC/DEC mixture was prepared and placed into several ampules that were then sealed and stored at 85 °C for varying lengths of time. During storage, all samples had some degree of darkening. The ^{11}B and ^{19}F NMR spectra, Figures 6 and 7, respectively, and the mass spectra showed an increased level of the BF_4^- anion relative to that of $LiIm(BF_3)_2$ and a new species that appeared as only a trace species in a fresh sample. The new peaks in the mass spectrum at 319 and 251 *m*/*z* are assigned to the new anion $BF_2(Im(BF_3))_2^-$, shown in eq 4 ($n = 0$), and the loss of one molecule of BF_3 from this anion, respectively. The ^1H NMR spectra,

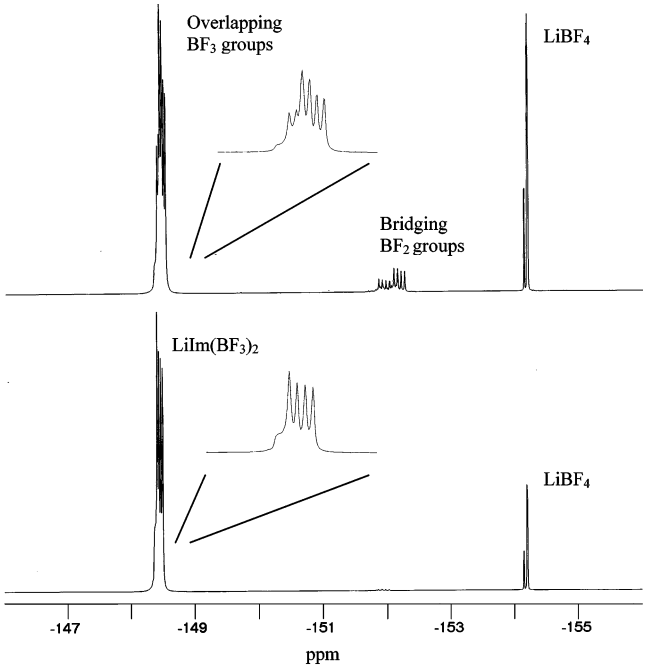

Figure 7. ^{19}F NMR spectra at 470.5 MHz of a 1 M LiIm$(BF_3)_2$ 1/1/1 EC/DMC/DEC solution before (bottom spectrum) and after (top spectrum) storage at 85 °C for 7 months in a sealed glass vial. The new species that form after storage at 85 °C (besides $LiBF_4$) have imidazole rings linked by BF_2 groups with the terminal imidazole groups having a BF_3 group whose ^{19}F NMR signal overlaps with that of LiIm$(BF_3)_2$.

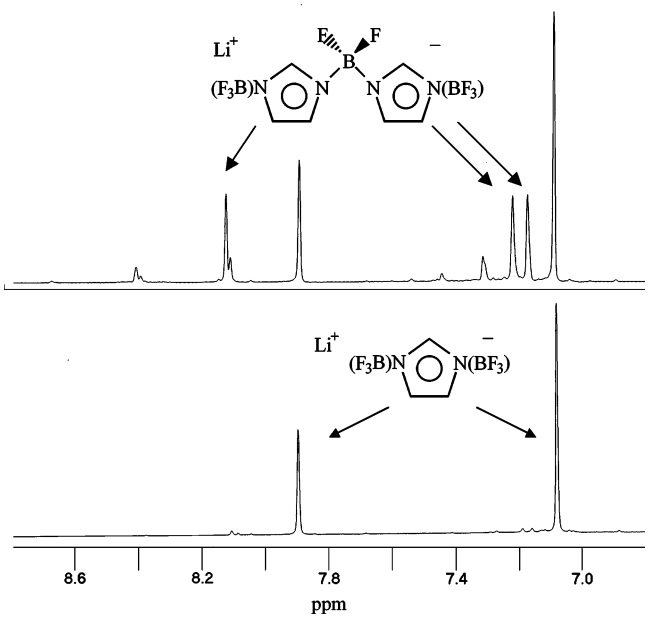

Figure 8. ^{1}H NMR spectra at 500 MHz of the aromatic region of a 1 M LiIm$(BF_3)_2$ 1/1/1 EC/DMC/DEC solution before (bottom spectrum) and after (top spectrum) storage at 85 °C for 7 months in a sealed glass vial. Unmarked peaks are presumably due to a species with two BF_2 groups linking three imidazole groups. (See the text.)

Figure 8, show the growth of a new species with a 1/1/1 integral ratio showing the loss of symmetry around the imidazole ring, consistent with the above assignment of the mass spectrum. The ^{11}B and ^{19}F NMR spectra of the stored sample clearly show overlapping 1/2/2/1 and 1/1/1/1 quartets ($J_{B-F} = 13$ Hz), respectively, that correspond to the BF_3 groups of new species and the starting salt. The BF_2 group is observed as one of the overlapping 1/2/1 triplets in the ^{11}B NMR spectrum and as a 1/1/1/1 quartet ($J_{B-F} = 26$ Hz) in the ^{19}F NMR spectrum, respectively. The other triplet and quartet ($J_{B-F} = 26$ Hz) in the ^{11}B and ^{19}F spectra, respectively, are assigned to a new species that appears as small peak at *m*/*z* 435 in the mass spectrum. This additional triplet and the lack of a doublet in the ^{11}B NMR spectrum show that the decomposition product with an *m*/*z* of 435 consists of three imidazole groups linked by two BF_2 groups with BF_3 groups capping the terminal nitrogen atoms, shown in eq 4 ($n = 1$), rather than $BF[Im(BF_3)]_3^-$, which would have the same mass. Presumably, the additional peaks in the ^{1}H NMR spectrum may be assigned to this species, and the terminal BF_3 groups overlap with the BF_3 groups of the other compounds in the ^{11}B and ^{19}F NMR spectra. Samples withdrawn at 3, 5, and 7 month intervals were all identical to each other, including their relative signal intensities in the NMR indicating that an equilibrium had been established. No decomposition was observed in a similar sample that was stored for 9 months at room temperature.

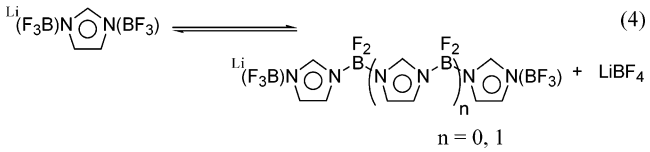

(4)

These results suggest that the decomposition of LiIm$(BF_3)_2$ occurs at elevated temperatures through ligand disproportionation as shown in eq 4. The mechanism is probably similar to one of the two mechanisms proposed by Hartman and Schrobilgen[14] for tetrahaloborate disproportionation to form mixed tetrahaloborate anions. In the present case, only one of the mechanisms is probable because the other mechanism requires the loss of a fluoride ion over that of an imidazolate fragment from the boron atom as a first step, which is unlikely. The most probable mechanism is shown below as the sequence in Scheme 1. The initial step is the loss of BF_3 from the anion. Abstraction of fluoride from an anion by BF_3 proceeds through a fluoride-bridged intermediate analogous to the known species $B_2F_7^-$ [15] to form $LiBF_4$. Recombination of the $(BF_3)ImBF_2$ with BF_3Im^- forms the bridged species.

Chain formation with BF_2 groups linking the imidazole groups is observed as a disproportionation product. Previously observed reactions between BF_3 and other anions possessing two Lewis base sites also show ligand disproportionation, but there was no evidence of chain growth.[16] In fact, for the acetate anion, continued replacement of fluoride with the acetate to form $BF(O_2CCH_3)_3^-$ was

(14) Hartman, J. S.; Schrobilgen *Inorg. Chem.* **1972**, *11*, 940.
(15) (a) Brownstein, S.; Paasivirta, J. *Can. J. Chem.* **1965**, *43*, 1645. (b) Harris, J. J. *Inorg. Chem.* **1966**, *5*, 1627.
(16) (a) Brownstein, S. *Can. J. Chem.* **1978**, *56*, 343. (b) Brownstein, S.; Latremouille, G. *Can. J. Chem.* **1978**, *56*, 2764.

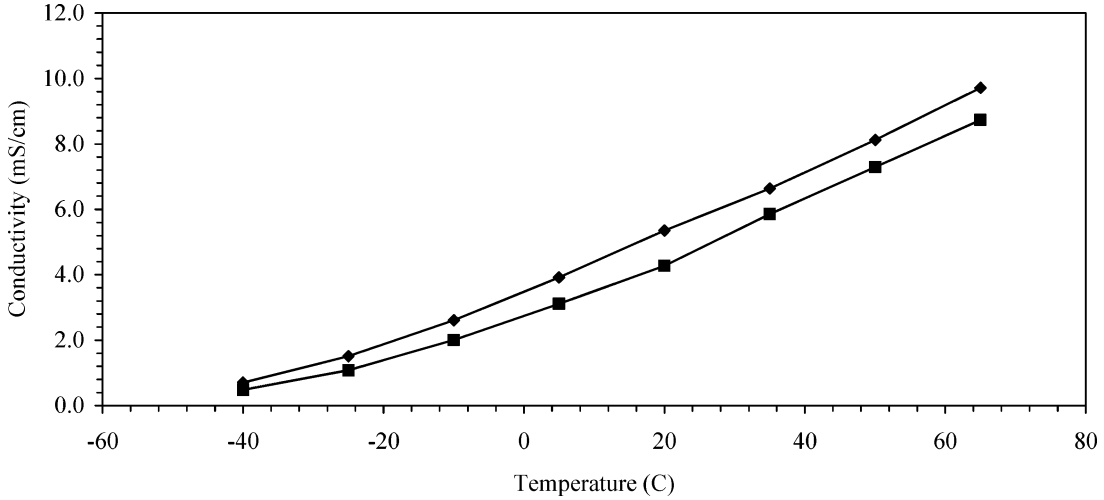

Figure 9. Comparison of the conductivity of a fresh (◆) 1 M $LiIm(BF_3)_2$ 1/1/1 EC/DEC/DMC (wt %) solution and the same solution stored (■) at 85 °C for 7 months.

Scheme 1. Mechanism for the Disproportionation of $LiIm(BF_3)_2$

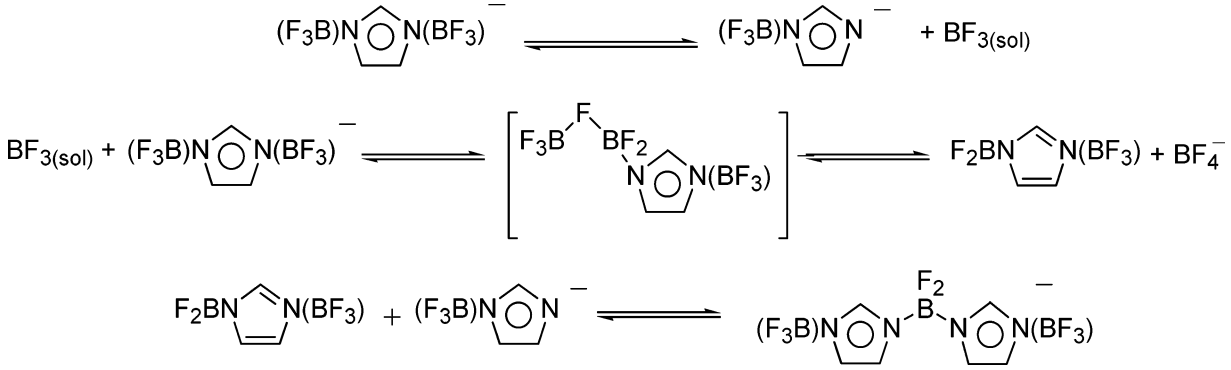

observed. According to the proposed mechanism, the disproportionation products, $BF[Im(BF_3)]_3^-$ and $B[Im(BF_3)]_4^-$, could form if fluoride were abstracted from the BF_2 or BF group of $BF_2[Im(BF_3)]_2^-$ and $BF[Im(BF_3)]_3^-$, respectively, to form their conjugate Lewis acids. For the intermediate conjugate Lewis acids $BF[Im(BF_3)]_2$ and $B[Im(BF_3)]_3$ to form, BF_3 must have Lewis acidity similar to or greater than these Lewis acids to compete effectively for fluoride. The fact that these products are not observed implies that BF_3 has a lower Lewis acidity than these conjugate Lewis acids. The lower Lewis acidity of BF_3 can at least be partially explained by the ability of the fluorine atoms to contribute significant electron density through its electron lone pairs to the formally empty 2p(π) atomic orbital of boron.[17] For an imidazolate fragment, $Im(BF_3)^-$, the electron lone pair that can contribute electron density to the empty 2p(π) atomic orbital of boron is also shared with the imidazolate ring to give it aromaticity. The imidazolate fragment is therefore a poor π donor, and as fluoride ligands are replaced with imidazolate fragments on the boron atom, fluoride abstraction by BF_3 becomes less favorable. Instead, fluoride abstraction occurs at a terminal BF_3 group of $BF_2[Im(BF_3)]_2^-$, which allows chain growth to occur. Steric effects should not interfere with the formation of $BF[Im(BF_3)]_3^-$ and $B[Im(BF_3)]_4^-$ because species with four imidazole groups around a single boron atom are known.[18]

In principle, it should be possible that polymeric chains with BF_2 groups linking imidazole groups could grow according to the above mechanism. However, this does not appear to occur to an appreciable extent. After sevens months of storage, only a tiny amount of an unidentified gel was observed at the bottom of the glass vial in which the solution was stored. This gel could potentially be a small amount of the polymer or it could simply be due to the settling of very fine particles that passed through the frit during the work up of the reaction. Furthermore, no species with more than three imidazole rings was detected in the mass spectrum, and only two types of BF_2 bridging groups corresponding to the species described above were detected by[19] F and ^{11}B NMR spectroscopy. The most reasonable explanation for the apparent lack of chain growth is that chain cleavage occurs between the BF_2 unit and the imidazole ring. As a polymer grows, there are a greater number of BF_2-Im sites at which cleavage of the polymer chain can occur, thus limiting its growth as shown below. In addition, the Lewis basicity of the imidazolate ligands should decrease as the negative charge is distributed over a larger molecule, thus weakening

(17) Cotton, F. A.; Wilkinson, G. *Advanced Inorganic Chemistry*, 5th ed; Wiley: New York, 1988; p 173.

(18) Chao, S.; Moore, C. E. *Anal. Chim. Acta* **1979**, *100*, 457.

(19) Ravdel, B.; Abraham, K. M.; Gitzendanner, R.; DiCarlo, J.; Lucht, B.; Campion, C. *J. Power Sources* **2003**, *119−121*, 805.

the B−N bonds leading to greater fragmentation as the polymer grows.

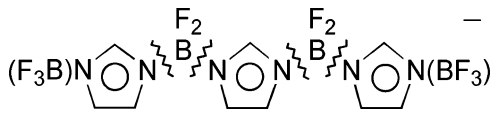

The disproportionation of the salt does lower the conductivity somewhat as shown in Figure 9. The conductivity of the salt at 20 °C decreases from 5.31 to 4.21 mS/cm after 7 months of storage at 85 °C. For comparison, a 1 M $LiPF_6$ electrolyte solution stored under similar conditions decomposes rapidly generating a precipitate, gas pressure, and the loss of 24% of its conductivity at 85 °C after 1 day.[19] The lower of conductivity of the stored solution of $LiIm(BF_3)_2$ is expected given that $LiBF_4$, a salt with a lower conductivity than $LiIm(BF_3)_2$, is formed. The other products of disproportionation, $LiBF_2[Im(BF_3)]_2$ and $Li[(BF_3)ImBF_2ImBF_2Im(BF_3)]$, although in all likelihood conductive and electrochemically stable salts, also contribute to an overall lower conductivity. This is because their large size can contribute to a higher solution viscosity that limits ion mobility. Nevertheless, the solution remains highly conductive and is not expected to become any less conductive with further exposure to high temperature because the system has established an equilibrium concentration. On the basis of these data, these new imidazolate-based salts might be "thermally stable" alternatives for $LiPF_6$ in organic carbonate-based electrolyte solutions for Li-ion batteries.

Conclusions

A series of Li salts of WCAs have been prepared from inexpensive starting materials using a simple synthetic process in high yield. The salts are highly conductive in organic carbonate solutions and may be used in Li-ion batteries. The new imidazole-based salts have high conductivity because of effective charge distribution of charge across the anion. Crystal structures were obtained that show that the anions form contact ion pairs with the lithium cation through their fluorine atoms. Similar contact ion pairing is probably present in organic carbonate electrolyte solutions used for Li-ion batteries. The lower conductivity of the amide-based salt solutions, $LiN(CH_3)_2(BF_3)_2$, relative to solutions containing imidazole-based salts is attributed to stronger ion pairing between the anion and lithium cation. Stronger ion pairing between the lithium cation and the $N(CH_3)_2(BF_3)_2^-$ anion is attributed to less effective anion charge distribution and chelation to the lithium cation which was observed in the solid-state structure. Thermal stability experiments show that after 7 months at 85 °C some decomposition by ligand disproportionation is observed in an electrolyte solution containing the parent imidazole-based salt. The products are lithium salts that are expected to be conductive and electrochemically stable in a Li-ion cell. The disproportionation does yield lower-conducting salts such as $LiBF_4$, which lowers the conductivity about 20% from that of the starting solution at room temperature. However, the conductivity is still high enough for commercial applications. The conductivity is not expected to decrease further because the system reaches equilibrium. Thus, although these new lithium salts partially decompose at elevated temperatures, the products of decomposition are not likely to be detrimental to Li-ion cell components. Future investigations will determine the compatibility of the disproportionation products in a Li-ion cell environment and if these new salts could be considered thermally stable alternatives to $LiPF_6$ despite their disproportionation at elevated temperatures.

Acknowledgment. This work was supported by the U.S. Department of Energy and the U.S. Air Force under contracts DE-FG 02-01ER83345 and F-33615-98-C-2898. We thank Dr. K. M. Abraham for his helpful advice.

Supporting Information Available: NMR and mass spectra, cell cycle life, and X-ray crystallographic data in CIF format including atomic coordinates, bond distances and angles, and anisotropic thermal parameters for $[LiBenzIm(BF_3)_2 \cdot 2EC]_2$ and $[LiN(CH_3)_2(BF_3)_2 \cdot H_2O)]_n$. This material is available free of charge via the Internet at http://pubs.acs.org.

IC040070X